



## A Novel Starch Nanoparticle Citrate Based Adsorbent for Removing of Crystal Violet Dye from Aqueous Solution



Ehab Gad<sup>1,2\*</sup>, Medhat Owda<sup>2</sup>, Ramadan Yahia<sup>2</sup>

<sup>1</sup> Chemistry Department, Faculty of Science and Arts, Jouf University, Saudia Arabia.

<sup>2</sup> Department of Chemistry, Faculty of Science, Al-Azhar University, Nasr City.

**P**REPARATION of corn starch by pullulanase to obtain starch nanoparticles (StNPs) with high yield and short duration was considered as the best way for green industry of StNPs as compared with other preparation procedures. Morphology investigation of prepared StNPs by scanning electron microscope (SEM), particle size by Dynamic light scattering (DLC) and Transmission electron microscope (TEM), group changing by Fourier transforms infrared spectroscopy (FTIR) and crystallinity by X-ray diffraction (XRD). Modification of StNPs via crosslinking with citric acid to obtain StNPs citrate. A novel adsorbent of obtained StNPs citrate was examined for dye-removing from aqueous solutions. Crystal violet dye was remediated with StNPs citrate to investigate the adsorption efficiency. Batch experiments were carried to study the optimum pH, contact time, adsorbent dose, initial dye concentration and temperature to assess the kinetic from isotherm of adsorption. The experimental data were best fitted to pseudo second order and Langmuir isotherms. Thermodynamic functions such as free Gibbs energy ( $\Delta G^\circ$ ), enthalpy ( $\Delta H^\circ$ ) and entropy ( $\Delta S^\circ$ ) of the sorption were calculated, thus indicated spontaneous and endothermic adsorption process.

**Keywords:** Starch nanoparticles, Crystal Violet, StNPs citrate, Thermodynamics.

### Introduction

In last decades scientists were begun seeking for raw materials fulfilled human requirements but at the same time ecofriendly. Replacement of petroleum-based materials and industrial chemicals used in human utilities become the greatest thinking and research of scientists because of two main reasons, availability and environmental concerns. Polysaccharides are a large number of this family and including a large number of biopolymers from various sources [1]. Starch has many features among other natural polymers (abundant, inexpensive, renewable, non-toxic and environment-friendly). An expansive sum of starch is delivered in stabilized crops like (potato, wheat, maize, rice, and cassava). Starch granules are made up of ample nano-sized semi-

crystalline squares. Through direct hydrolysis utilizing acids and/or proteins, the nano-blocks might be separated from starch. At most starch granule is composed of amylose and amylopectin which are different in structure chain. Amylose is a linear structure of glucose units with molecular weight nearly a million linked by  $\alpha$ -(1-4) glucosidic bond. Amylopectin is a linear chain of glucose units linked by  $\alpha$ -(1-4) glucosidic bond and branches linked by  $\alpha$ -(1-6) glucosidic bond and molecular weight up to hundred million. Recently a universal review published on starch nanoparticle preparation, characterization and applications [2]. Starch nanoparticles have pulled in analysts in final decades since of solitary physicochemical properties as compared with local starch [3]. Starch nanoparticles have promising future in numerous mechanical applications as an antioxidant [4], bundling,

\*Corresponding author e-mail: e\_said56@yahoo.com

Received 5/9/2018; Accepted 14/11/2019

DOI:10.21608/ejchem.2019.16593.2013

©2020 National Information and Documentation Center (NIDOC)

papermaking industry [5], a carrier in drugs [6], adsorbent in wastewater treatment [7, 8] and at last as moderate discharge fertilizer [9]. Dyes are the most serious environmental issues that many industrial processes, such as cosmetics, textiles, paper, food, printing, plastics, pharmaceutical and leather, have put into the environment [10]. Even at very low levels-highly visible-water coloring is unacceptable and must be eliminated before the sewage is discharged into the environment [11]. Nevertheless, due to their complex aromatic molecular structures and high water solubility, dyes are quite difficult to biodegrade and remove from dye wastewater [12]. Crystal violet has dangerous effects on small periods of exposure on living organisms. Crystal violet is commonly used in veterinary medicine as an animal drug. In contrast, the detection of bloody fingerprints is used as a biological dye. It is unhealthy for humans and, if eaten or inhaled, can cause cancer [13]. This work aims to prepare starch nanoparticles from corn starch by pullulanase as isoamylase by self-assembly at 40 °C. A novel great adsorbent was arranged from crosslinking starch nanoparticles with citric corrosive for the expulsion of Precious Crystal Violet dye from the watery arrangement.

## Experimental

### Materials and methods:

Corn starch from Egyptian starch and Glucose Company ESGC, Pullulanase was supplied by GENENCORE, Citric acid, Hydrochloric acid,

Caustic soda and Disodium hydrogen phosphate were provided by Sigma Aldrich. All chemicals are explanatory review.

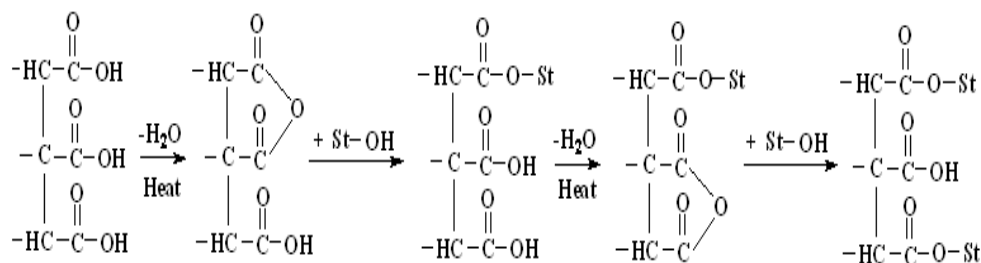
### Preparation of starch nanoparticles

Starch slurry 5 % was arranged in buffer pH (4.6) by weighing 10 gm native corn starch and suspended in a buffer solution in measuring flask 250 ml, then, put in beaker 500 ml and stirred for 30 min in boiling water bath on the hot plate and stirring at 1200 rpm till gelatinized starch obtained. To adjust the temperature of the slurry to add the enzyme, the water bath temperature was decreased to 58 °C. The concentration of enzyme has been added 30 ASPU/ g starch to start the reaction of debranching of chains of glucans in amylopectin at 58 °C and stirring at 300 rpm for 8 hrs. The temperature then rose to 100 °C for 30 min to stop the reaction of debranching. Later, the slurry was cooled to room temperature then stored at 4 °C for 8 hrs. for recrystallization of debranched glucans chains occurred. Finally, the recrystalline starch washed by distilled water and centrifuged 4 times till neutrality, put in lyophilizer at 4 °C to complete drying the StNPs and weighed to calculate the percentage of yield as following [3]:-

$$\text{Yield \%} = \frac{\text{weight of freeze-dried StNPs}}{\text{initial weight of native starch}} \times 100$$

### Preparation of StNPs citrate.

The citric acid solution was prepared as



**Scheme 1. Dehydration of citric acid then reacted with StNPs.**

shown in **Scheme 1** by dissolving 3 g citric acid in 30 ml of ethanol, then 20 ml of the prepared solution mixed with 2 g StNPs in a petri dish and conditioned for 12 h at room temperature to allow the complete intake of a citric acid solution by StNPs. The Petri dish was dried in the oven at 50 °C for removing ethanol and then heated in the oven at 130 °C for 4 hrs. for ending the reaction. The modified StNPs washed three times with water to remove citric acid impurities, then with ethanol to remove water and dried at room temperature and finally ground [14].

#### Characterization

##### Scanning electron microscopy (SEM)

Sticky tape (native starch) and carbon coat (StNPs) were used to mount native starch and StNPs specimens on carbon sample holders. They were watched employing a Quanta 250 FEG(Field Outflow Weapon) filtering electron magnifying instrument (Made in Britain) with the SEM mode at 30 kV quickening voltage. Micrographs were presented at 3000 and 30000 magnification for (native starch) and (StNPs) respectively.

##### Transmission electron microscopy (TEM)

Transmission electron micrographs of StNPs were taken with a JOEL-JEM 1010 transmission electron microscope (Made in Japan) with an acceleration voltage of 80 kV. StNPs were stored on a carbon-coated network without any medications.

##### X-ray diffraction (XRD)

Native starch and StNPs samples have stayed for 24 hrs. in a sealed container at 85% relative humidity to achieve constant moisture content. XRD patterns were measured at room temperature. A Siemens D-5000 diffractometer (BRUKER, D8, Germany) using Cu Ka radiation ( $k = 1.543$ ) and an auxiliary bar graphite monochromator was turned on at 40 kV and 30 mA.

##### Dynamic light scattering (DLS)

The size of StNPs was determined using DLS at room temperature on a Plus particle size analyzer (Nicomb Instruments Corporation) at the 90 scattering angle (Calif., USA). All test arrangements were sifted utilizing expendable

0.45  $\mu\text{m}$  pore channels earlier to examination at a concentration of 1.0 mg/ml.

##### Fourier transforms infrared spectroscopy (FTIR)

Fourier transforms infrared spectra of corn starch, StNPs and StNPs citrate were acquired on FTIR spectra (Japan-JASCO 4600) using KBr disk technique. The tests were compressed into lean disk-shaped pellets for FTIR estimation after blending with anhydrous KBr. The spectra were gotten with a determination of 2  $\text{cm}^{-1}$  between wave number ranges of 4000 - 400  $\text{cm}^{-1}$ .

##### Adsorbate preparation and calibration

A stock arrangement of Crystal Violet dye was arranged by dissolving 0.125 g in 500 ml of distilled water to obtain 250 mg/l color concentration arrangement. The working concentrations were prepared by diluting 250 mg/l predetermined volumes of the stock solution accurately to known initial concentrations of 100-500 mg/l. A calibration curve of the Crystal Violet dye was first prepared via serial dilution and absorbance determined using a UV-spectrophotometer (T80+ UV/Vis spectrometer) at  $\lambda_{\text{max}} = 584$  nm. All absorbance readings are measured in duplicate and the average absorbance values of Crystal Violet dye calculated.

##### Batch sorption examination

Examination of Sorption through single batch reactor systems were carried out and the effects of different parameters such as; StNPs citrate adsorbent dosage (10-50 mg), pH (2.5-10.5), initial dye concentration (100-500mg/l), temperature (25-55°C) and effect of contact time (10-240 min.) were studied. The sorption experiments were performed at constant agitation speed of 300 rpm using 50 ml beaker containing 20ml of Crystal Violet dye solution of known concentrations. pH solutions were adjusted with either 0.1M HCl or NaOH. Determination of equilibrium between StNPs citrate and Crystal Violet dye by shaken the beaker for different time intervals till reach an adequate time. StNPs citrate Sorption capacity screened at known time intervals to measure the residual dye concentration using UV-V is spectrophotometer at  $\lambda_{\text{max}}$  of 612 nm. The quantity of dye absorbed at equilibrium was then determined using Eq. (1) [15]:

$$q_e = (C_0 - C_e) \times V / M \quad (1)$$

where,  $q_e$  (mg/g) is the equilibrium adsorption capacity of adsorbed dye onto StNPs citrate,  $C_0$  (mg/l) the initial concentration of Crystal Violet dye,  $C_e$  (mg/l) the equilibrium concentrations of dye in liquid phase,  $V$  (L) the volume of dye solution and  $M$  (g) the mass of StNPs citrate used. The percentage of Crystal Violet dye removal was also calculated using Eq. (2) [16]:

$$\text{Removal \%} = (C_0 - C_e) / C_0 \times 100 \quad (2)$$

where,  $C_0$  (mg/l) is the initial concentration of Crystal Violet dye and  $C_e$  (mg/l) the equilibrium concentration of dye at time,  $t$ .

## Results and Discussion

### *Characterization of prepared StNPs and StNPs citrate.*

#### *Morphology of native starch and StNPs*

The SEM and TEM images showed that the native starch and StNPs have a round and polyhedral shape as obtained by other studies [5]. The SEM images found in **Fig. 1a,b** indicate that the native corn starch has globular, polyhedral shapes with diameters of approximate 5–25  $\mu\text{m}$  and in **Fig. 1c,d,e** no apparent deficiency or hint of damage on the surface after debranching and recrystallization. The TEM images in **Fig. 1f,g,h** showed the well dispersed of StNPs with slight aggregation and diameter around 25–50 nm less than obtained from waxy maize (50–100 nm width and 80–120 nm length). After enzymolysis of residential starch, StNPs were shaped basically due to recrystallization of direct glucans (DP approximately 12–60). The linear glucans were easily fastidious deterioration. Therefore, the synthesizing process of StNPs through recrystallization had two steps: first, connecting linear glucans into double spirals and forming clusters with hydrogen bond; then, the modification of clustering into StNPs. After 8 h of debranching, twofold helices were likely amassed to nanoscale starch particles (25–50 nm, breadth) amid the 8 h recrystallization period. The impacts of freeze-drying on the arrangement of dried starch nanoparticles were impressive. The size of the particle more than 100 due to the aggregation of some particles as shown in other studies [3].

#### *Particle size of starch nanoparticles (StNPs)*

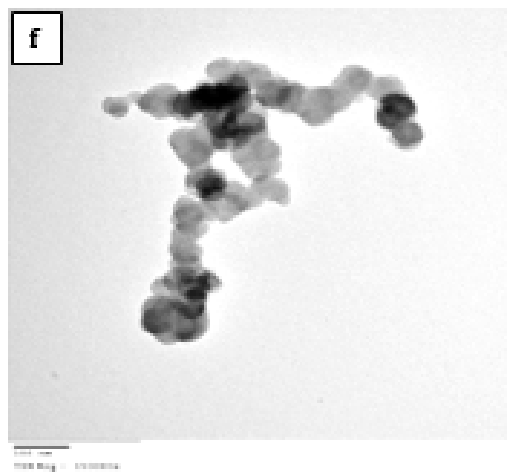
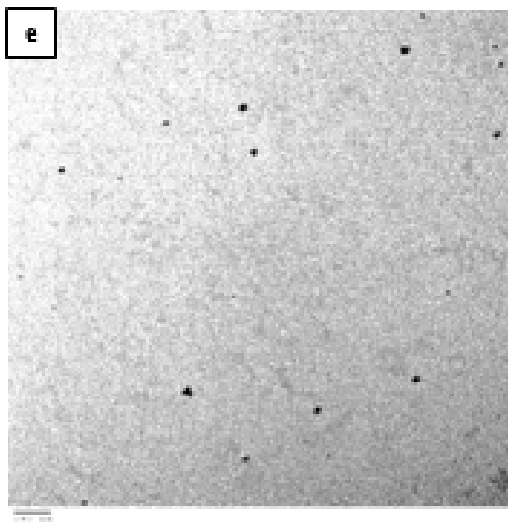
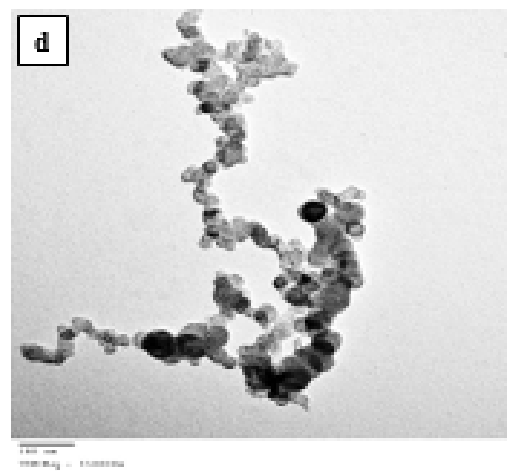
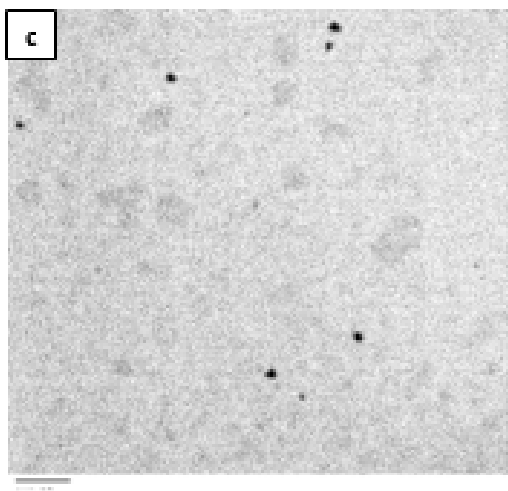
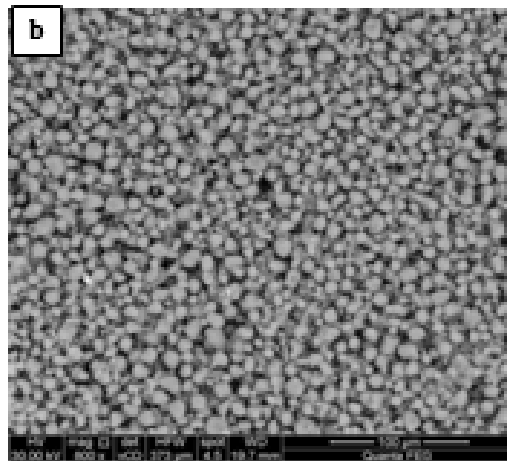
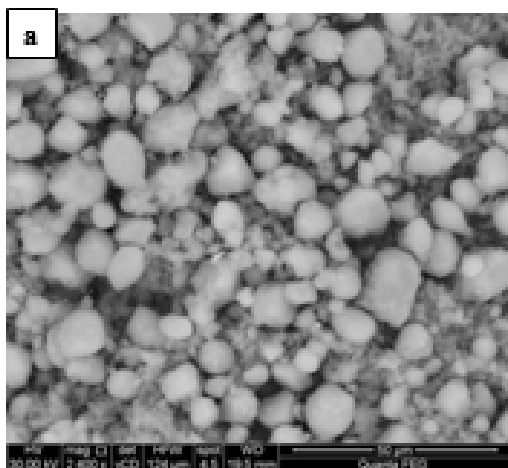
The estimate dissemination of StNPs was too measured utilizing DLS. As watched in **Fig. 2**, the estimate extended from 50 to 250 nm with about 100 nm as a cruel estimate, which was bigger than that measured by TEM. All through DLS estimation, there's an affinity of nanoparticles to aggregate in fluid state subsequently giving the measure of clustered particles instead of person particles. Unlike TEM, the results of the DLS resulted in a wider range of nanoparticles because this technique cannot be used to differentiate between individual particles and agglomerates. Similarly, it is observed that the TEM size was smaller than the DLS measurement results that could be attributed to nanoparticles self-aggregation [17].

#### *X-ray diffraction*

The crystalline structure of starch nanoparticles was examined by X-ray diffraction patterns to know the effect of the self-assembling procedure on crystallinity. Native corn starch granules had a typical A-type crystalline arrangement, showing diffraction peaks at around 15.8, 16.9, 18.1, and 23.5 (2 $\theta$ ) **Fig. 3**, in agreement with previous returns [18]. There were no changes in the X-ray of StNPs samples as compared with domestic starch exhibit a typical A-type crystalline structure with main diffraction peaks at 2 $\theta$  = 15.4, 17.1 and 22.5. This result may be due to the amylose content in corn starch 20–30% [5]. StNPs from native waxy maize (its amylose content 1–5%) gives different results according to the temperature of recrystallization [3, 17].

#### *FT-IR characterization*

The infrared spectra of local corn starch, StNPs, StNPs citrate are given by **Fig. 4**. Changes in FT-IR spectra for local maize starch and StNPs can be partitioned into band narrowing and changes in particular band retention concentrated. Band narrowing is caused by polymer requesting and a diminish within the number of conformations, whereas changes in band concentrated are caused by changes in particular conformations, such as long-range asking and crystallinity. As showed up in **Fig. 4a** wide groups from 3100 to 3700  $\text{cm}^{-1}$ , which were credited to the complex vibrational extend related with free, connect- and intra-molecular hydroxyl bunches. Bunches of 2925 and 2926  $\text{cm}^{-1}$  were characteristic of C–H amplifies related to the ring methane hydrogen



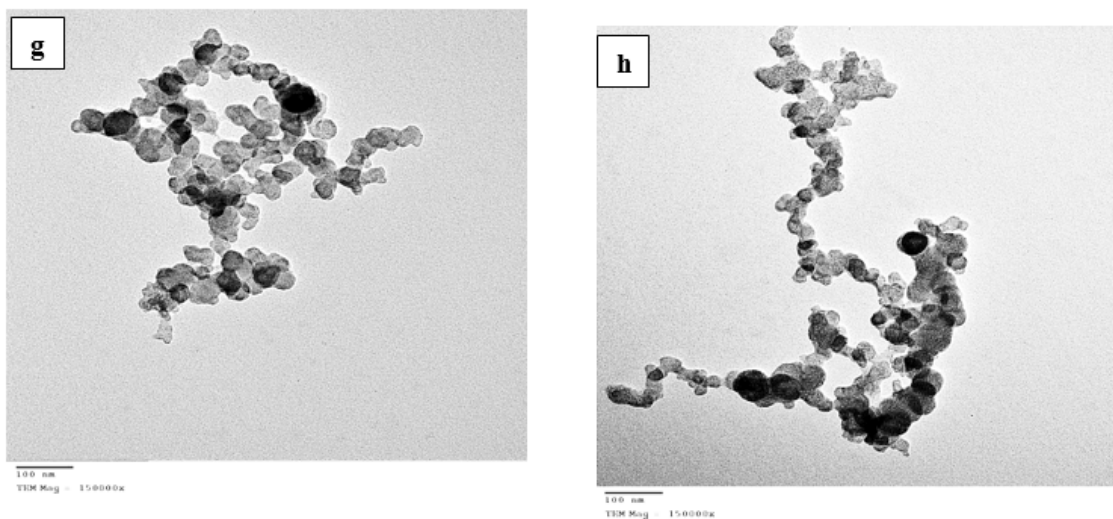


Fig. 1. SEM images (a, b) native starch. (C, d, e) StNPs. TEM images of StNPs. (f&g&h).

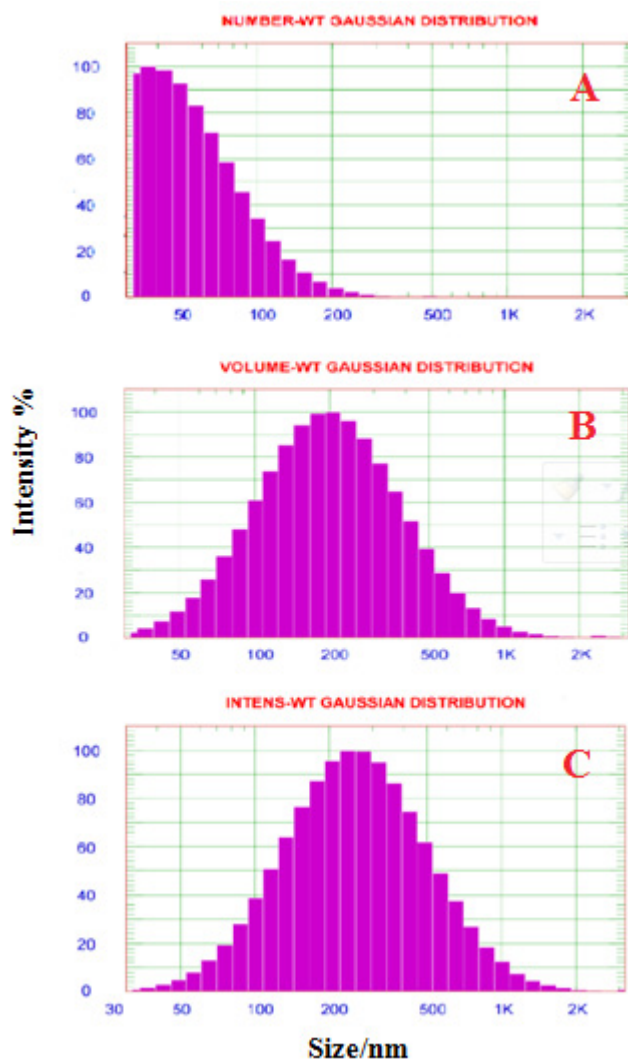


Fig. 2. Dynamic light scattering of StNPs after debranching and recrystallization of short glucan

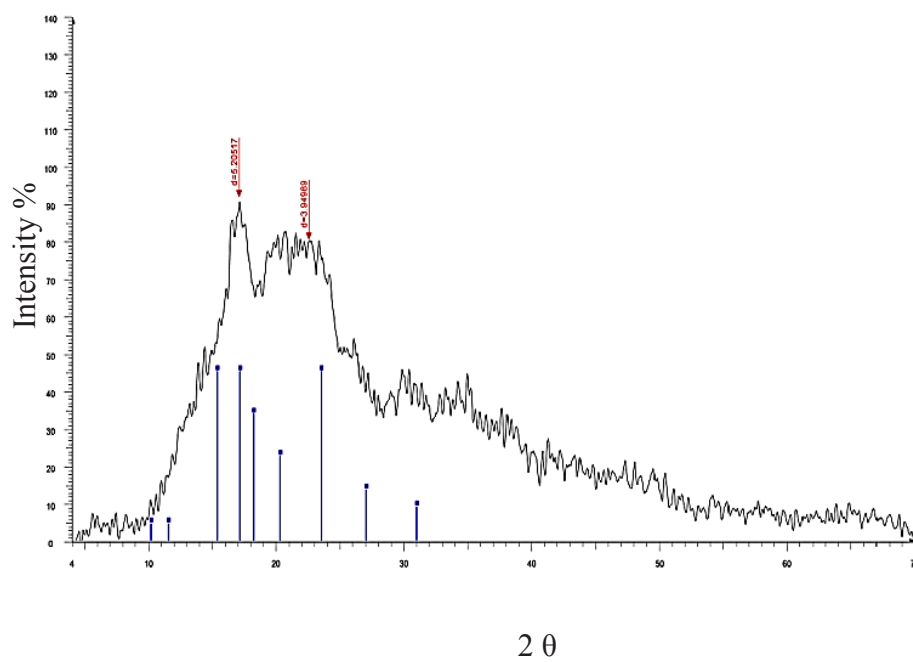


Fig. 3. XRD of StNPs

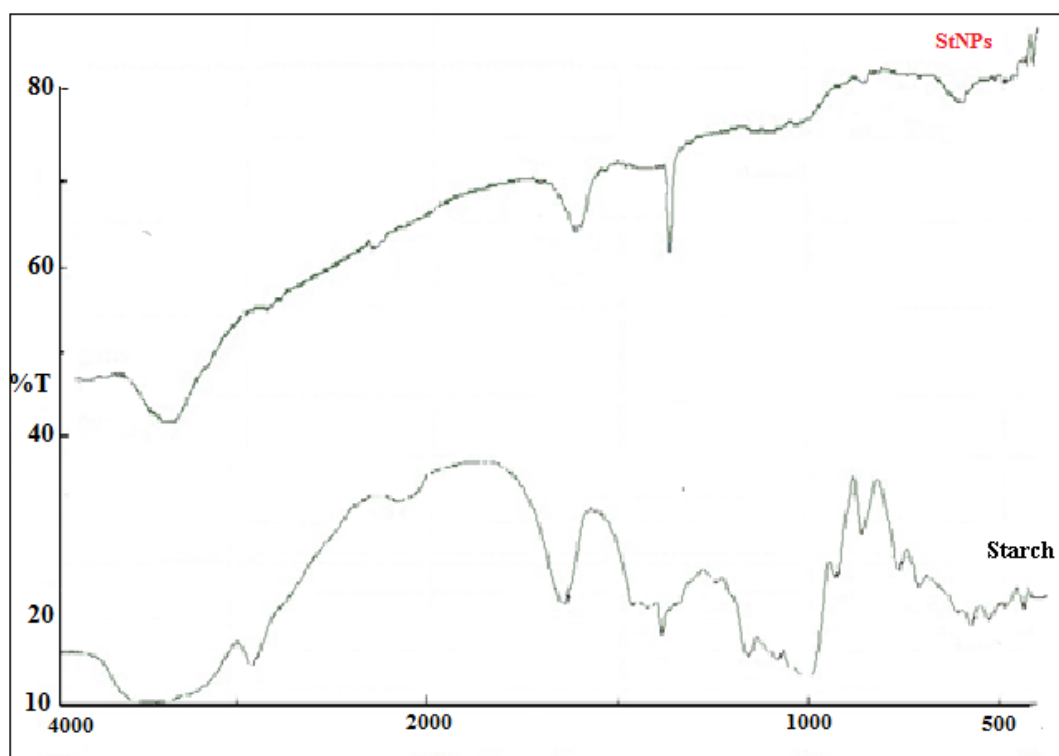


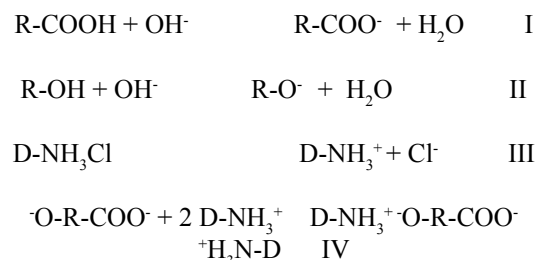
Fig. 4a. Starch and StNPs.

atoms. Due to the extending vibration of C–H and C–C bonds, the frail band at  $2077\text{ cm}^{-1}$ . An include of tightly-bound water was the top at  $1640\text{ cm}^{-1}$ . The top stature at  $1640\text{ cm}^{-1}$  was decreased compared to local starch and the width of the crest got to be more extensive. As shown in **Fig. 4a**, There were more differences in the region of fingerprints. Bands at wavelengths of  $1300\text{--}900\text{ cm}^{-1}$  have been reported to be sensitive to starch. The bands in this region are primarily the result of highly coupled vibrational modes of C–O and C–C. This coupling makes assigning individual bands difficult. Three characteristic crests showed up within the local starch range between  $933$  and  $1156\text{ cm}^{-1}$ ; these crests were credited to C–O bond extending. The escalated at  $940\text{ cm}^{-1}$  was ascribed to the skeletal mode vibrations of  $\alpha$ -1,4-glycosidic linkage (C–O–C). The crests at  $1081$ ,  $1156$ , and  $1020\text{ cm}^{-1}$  were characteristic of the anhydrous glucose ring C–O extend. On the off chance that there were appreciable band shifts within the FTIR spectra of the fabric, a particular chemical interaction (hydrogen-bonding) existed between the atomic chains. The lower the crest recurrence was, the more grounded the interaction was. Within the StNPs test appearing hydrogen bonds between starch atomic chains, the crests at  $1156$ ,  $1081$ , and  $1020\text{ cm}^{-1}$  in local starch moved to a lower recurrence of  $1150$ ,  $1078$ , and  $1015\text{ cm}^{-1}$ . In the method of enzymolysis  $\alpha$ -1, 6-glycosidic bonds were hydrolyzed and hydroxyl bunches were made and after that hydrogen bonds were shaped. Observing these shifts suggested that pullulanase had removed the native starch, which could increase the amount of linear glucans [3]. For StNPs cross-linked with citric corrosive starch-citrate subsidiary is shaped when citric corrosive was dried out to surrender an anhydride, which seem to respond with starch. A molecule of citric acid forms an effective interconnection between two starch molecules when a carboxyl terminal esterifies [18]. Conspire 1 given the schematic representation of the crosslinking response between starch and citric corrosive. FT-IR spectra of adjusted starch nanocrystals and citric corrosive appeared clear signs of alter. Unadulterated citric corrosive within the FT-IR range **Fig. 4b** The crest was  $1709\text{ cm}^{-1}$  due to the extending vibration of C=O in carboxyl bunches and the top was  $1743\text{ cm}^{-1}$ . It was a peak of interference that may well be found when carboxyl bunches were exceptionally near to each other in diacid [19]. However, the characteristic peaks at  $1709\text{ cm}^{-1}$  and  $1743\text{ cm}^{-1}$  disappeared after washing the modified starch

nanocrystals thoroughly with water. 4b. I don't know. For starch nanocrystals modified by citric acid, a clear new peak was found in the spectra at  $1732\text{ cm}^{-1}$ . since this crest is related with C = O ester extend and the adjusted starch nanocrystals have been altogether washed to expel the unbound citric corrosive, the nearness of the top of the ester carbonyl groups affirms the chemical linkage between starch and citric corrosive. The alter within the crest position within the altered starch nanocrystals from  $1709\text{ cm}^{-1}$  in immaculate citric corrosive to  $1732\text{ cm}^{-1}$  appeared that the crosslinking adjustment between starch and citric corrosive happened amid high-temperature warming [19]. The FT-IR results suggested that after modification, new interactions were formed between starch and citric acid. The C=O peak area ratio at  $1732\text{ cm}^{-1}$ . A degree of substitution was decided for the zone proportion of C = O top at  $1732\text{ cm}^{-1}$  to Goodness crest at  $3379\text{ cm}^{-1}$  in FT-IR spectra, i.e. the average number of hydroxyl groups substituted per glucose unit) of starch DS values of the starch nanocrystals modified with citric acid at  $130\text{ }^\circ\text{C}$  for 4hrs [18, 19].

#### Adsorption Examination

For Crystal Violet dye onto StNPs citrate cationic amine group of dye dissolved in aqueous solution attracted with carboxylate anion in StNPs citrate adsorbent as shown in **Scheme 2**.



**Scheme 2**

#### Effect of pH

Adsorption behaviors of crystal violet on StNPs citrate adsorbent were observed in the curves according to pH range in **Fig. 5a, b**. At pH values less than 2.5, the overabundance of protons ( $\text{H}^+$ ) competes with the Crystal Violet cationic bunches for the adsorption locales. Furthermore, carboxyl group ionization was suppressed at this pH, which weakened the electrostatic attraction between adsorbent and Crystal Violet molecules.

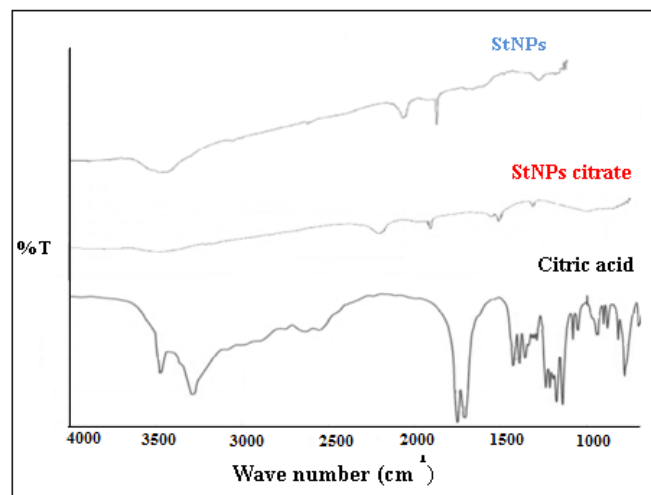


Fig. 4b. StNPs, Citric acid and StNPs citrate

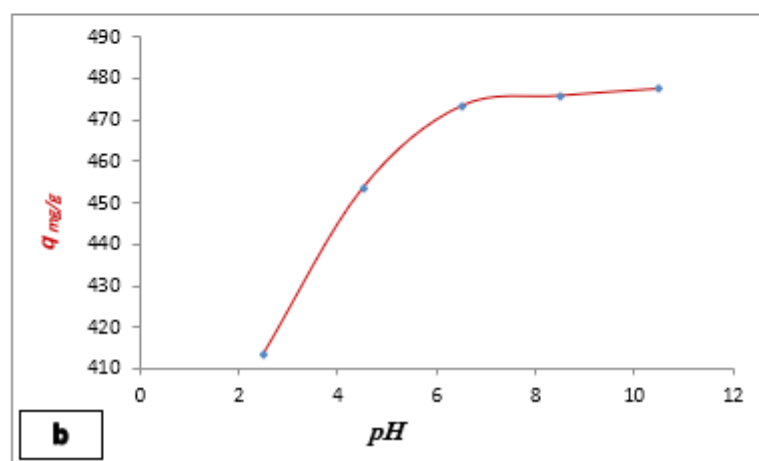
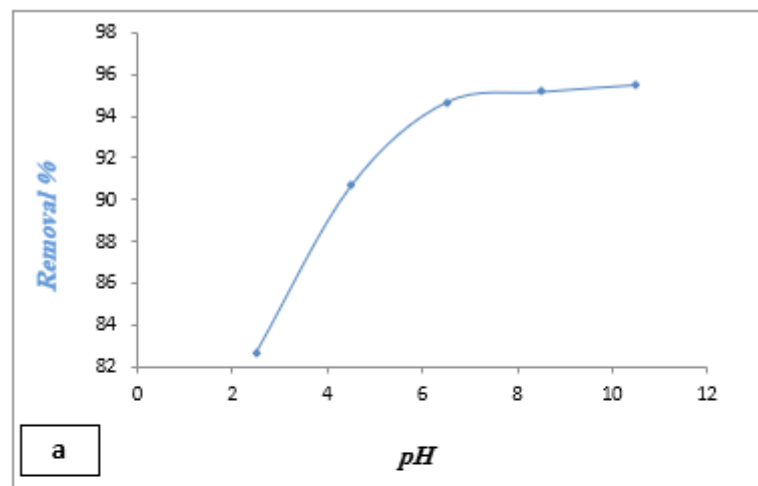


Fig. 5. Effect of pH on a, Crystal Violet removal percentage.

b, Crystal Violet adsorption capacity

The pH increasing from 2.5 to 10.5 promoted an adsorption process. For instance, the adsorption capacity of StNPs citrate increased from 413.3 to 473.3 mg/g at pH 8.5 close to the pKa of carboxyl groups, the negative charge density within StNPs citrate adsorbent increased and the adsorption capacity was enhanced. Therefore, pH 8.5 was established as optimal for further experiments as reported in another study [20, 21].

#### *Effect of adsorbent dose*

The adsorption capacity of StNPs citrate as a function of the dose was estimated at a different adsorbent dose (10-50mg), at constant 300 mg/l initial dye concentration, pH 8.5 and temperature of 25 °C for 120 min. The percentage of dye removal increased from 90 to 97.7% as the adsorbent dose increased from 10 mg to 50 mg, this increase was due to an increase in adsorption sites as StNPs citrate dose increased. as monitored in **Fig. 6a** where's the adsorption capacity of dye increased as adsorbent quantity increased until equilibrium then start to decrease as appeared in **Fig. 6b** as detailed in another consider [22].

#### *Effect of contact time*

The adsorption capacity of StNPs citrate and the removal of Crystal Violet dye were increased with time until reach equilibrium at 120 min. The experimental data screened in **Fig. 7a,b** at constant 300 mg/l initial dye concentration, constant adsorbent dose 30 mg/l, pH 8.5 and temperature of 25 °C as detailed in another consider [23].

#### *Effect of co-existing inorganic salts*

The effects of these salts (NaCl, Na<sub>2</sub>CO<sub>3</sub>, and K<sub>2</sub>SO<sub>4</sub>) on the adsorption of used dye onto StNPs citrate were studied at constant initial dye concentration (300 mg/l), constant adsorbent dose (30 mg/l), pH 8.5 and temperature of 25 °C for 120 min. They have inhibition effect on the adsorption process because these ions can screen the charged sites of the adsorbents leading to a suppression of the electrostatic interactions. The order of inhibition Cl<sup>-</sup> > CO<sub>3</sub><sup>-2</sup> > SO<sub>4</sub><sup>-2</sup> as shown in **Fig. 8a,b** as reported in another study [24].

#### *Effect of initial dye concentration*

Utilizing tall introductory color concentration, the impressive driving drive come about within

the dye's open-air mass exchange resistance between the fluid and strong stages, subsequently expanding sorption. Expanding introductory color concentration too leads to expanded collisions between color and adsorbent, hence moving forward the method of sorption. The impact of increasing the starting color concentration from 100 to 500 mg/l at steady arrangement pH (8.5), adsorbed measurements 30 mg/l and temperature of 25 °C at different times till equilibrium. **Fig. 9a** showed decreased in dye removal as initial dye concentration increased. The percentage decreased from 98.3% to 87.8% as dye concentration increased from 100 to 500 mg/l. Adsorption capacity increased from 163.8 to 731.6 as initial dye concentration increased from 100 to 500 mg/l as in **Fig. 9b** as reported in another study [25].

#### *Effect of Temperature*

Practically the adsorption capacity and dye removal calculated at constant initial dye concentration, adsorbent dose (300 and 30 mg/l respectively) and pH 8.5 at different temperatures (25, 35, 45, 55 °C) for 120 min. were shown in **Fig. 10a, b**. It can also be noted that with increase in temperature the percentage removal of Crystal Violet dye was found to be increasing. This can be attributed to the strong bond between the dye molecules and the binding sites of StNPs citrate, at higher temperatures. Biosorption was increased at higher temperatures as a result of the solution's increased surface activity and kinetic energy as reported in an earlier study [26].

#### *Adsorption isotherm*

Applying the most common models of Langmuir and Freundlich isotherms to demonstrate which of them suitable for adsorption isotherm of Crystal Violet dye adsorbed onto StNPs citrate adsorbent. Langmuir and Freundlich isotherms models are expressed by the Eqs. (3) and (4) respectively.

$$C_e/q_e = 1/bq_m + q_e/q_m \quad (3)$$

$$\log q_e = \log k_f + 1/n \log C_e \quad (4)$$

where  $q_e$  is the adsorption capacity (mg/g) at balance and  $q_m$  is the monolayer adsorption capacity per unit mass of adsorbent (mg/g) and  $C_e$  is the color concentration at equilibrium (mg/l). The parameter  $b$  is the Langmuir constant (l/mg),  $k_f$  is the Freundlich constant (l/g) and the parameter  $1/n$  (dimensionless) correlates the

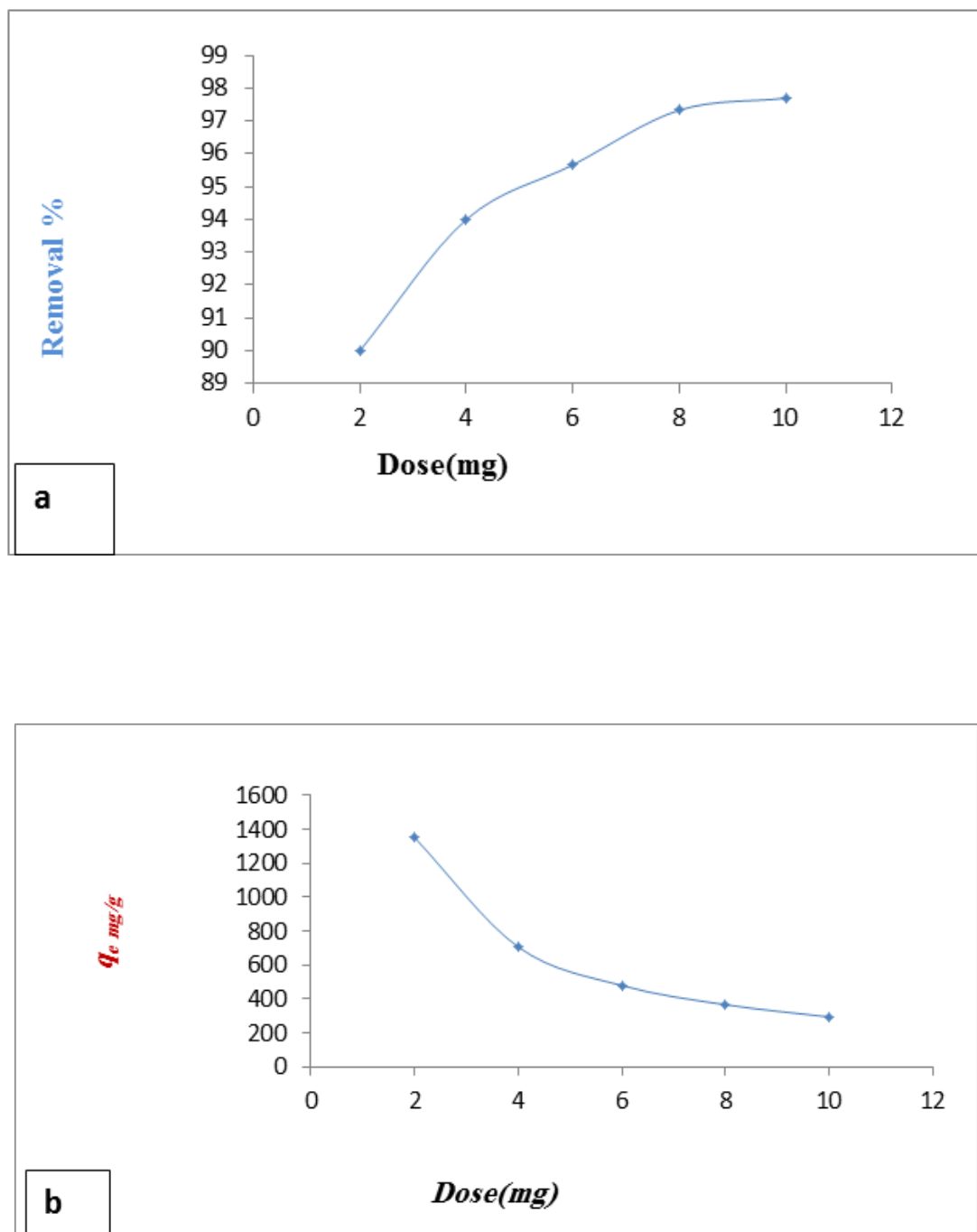


Fig. 6. Effect of adsorbent dose on a, Crystal Violet removal percentage.b, Crystal Violet adsorption capacity.

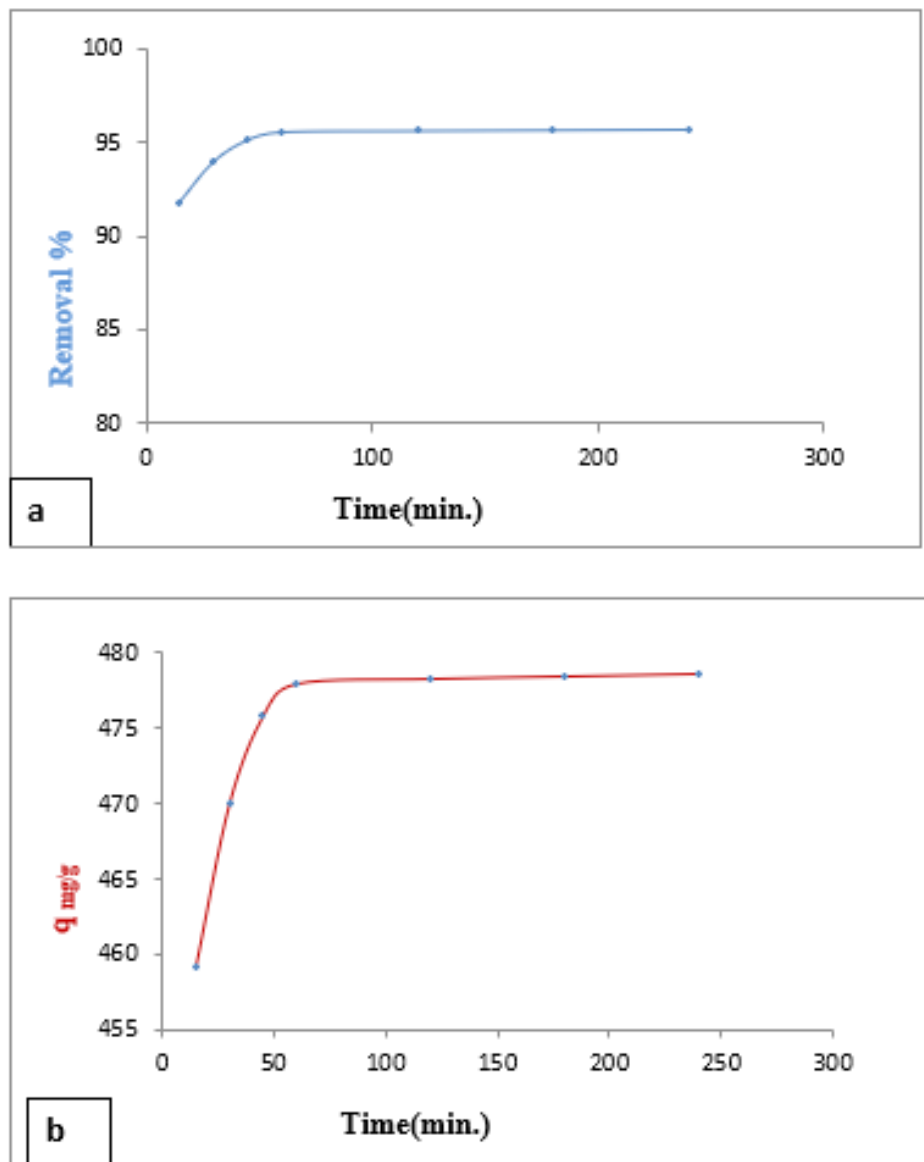


Fig. 7. Effect of contact time on a, Crystal Violet removal percentage.  
b, Crystal Violet adsorption capacity.

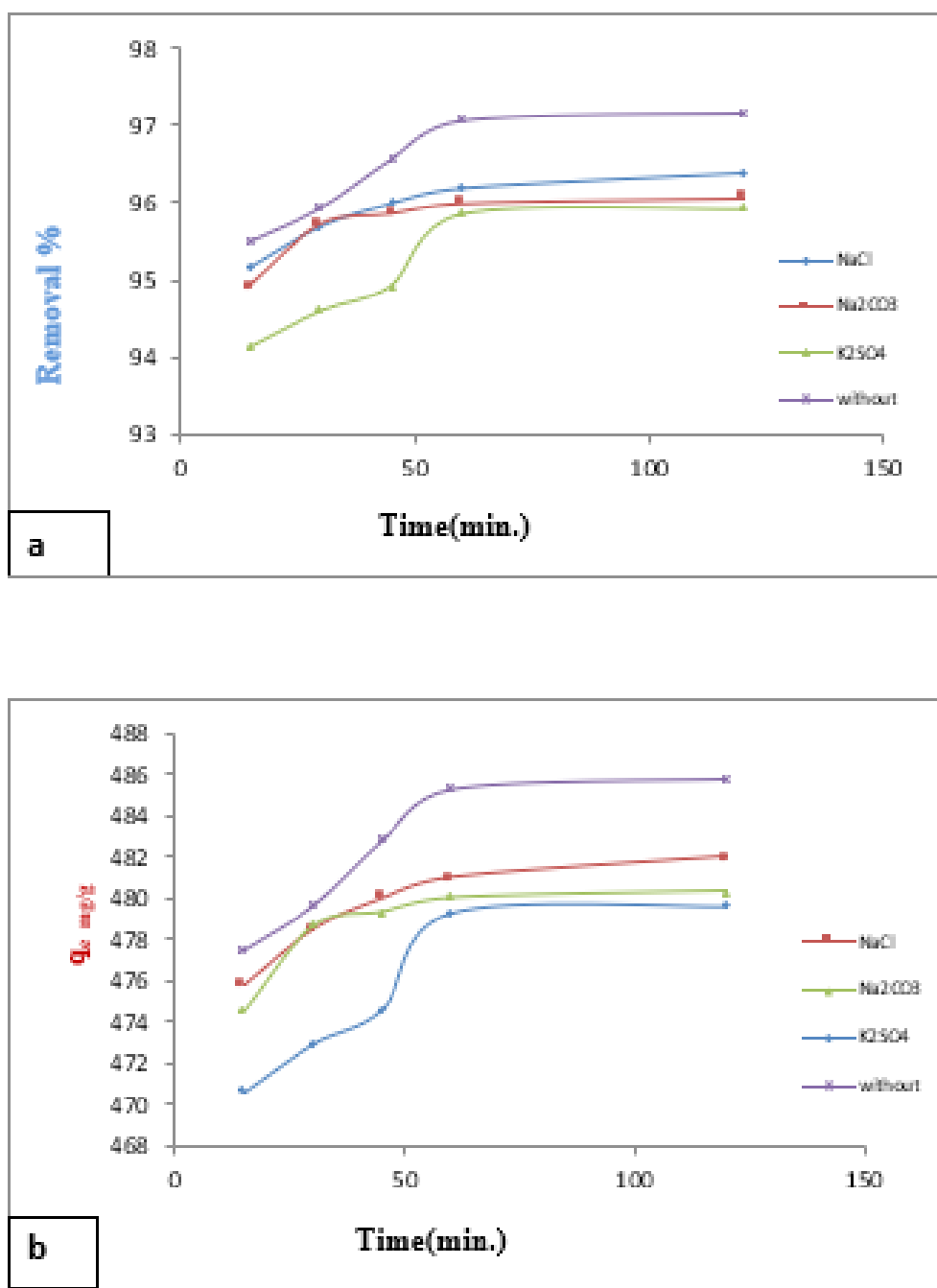


Fig. 8. Effect of inorganic salt on a, Crystal Violet removal percentage.

b, Crystal Violet adsorption capacity.

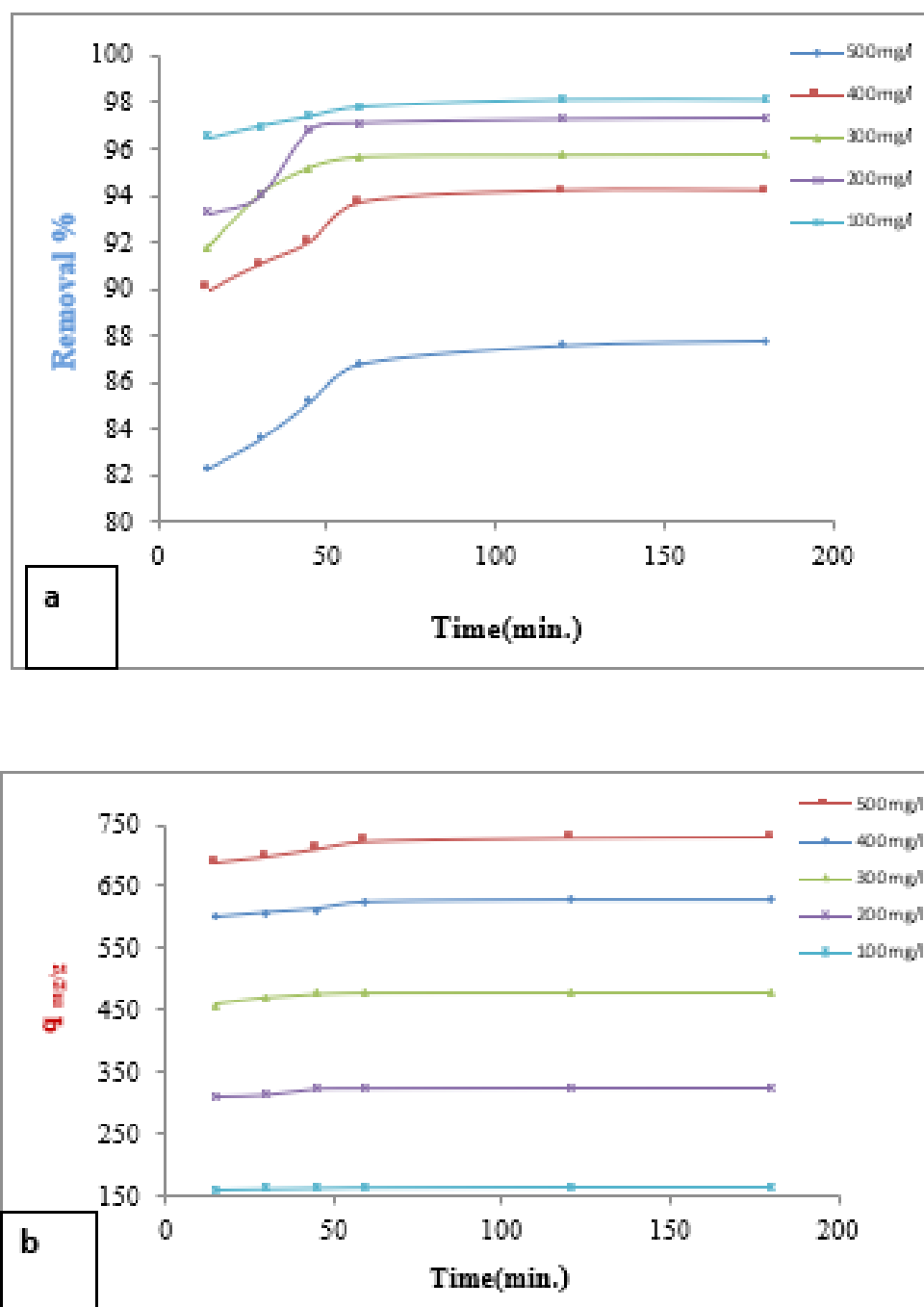


Fig. 9. a, Effect of initial concentration on Crystal Violet removal percentage.

b, Crystal Violet adsorption capacity.

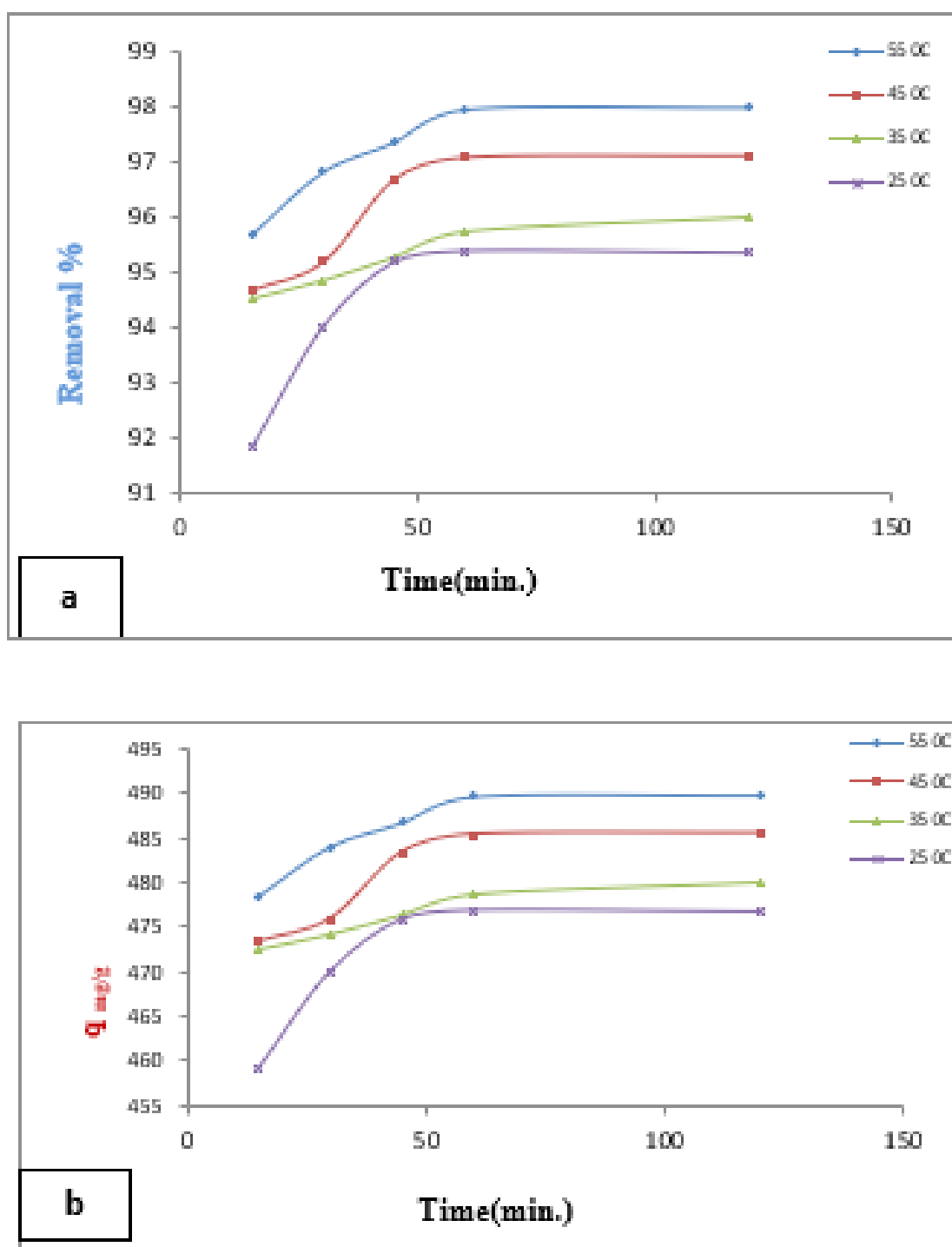


Fig. 10. Effect of temperature on a, Crystal Violet removal percentage.

b, Crystal Violet adsorption capacity.

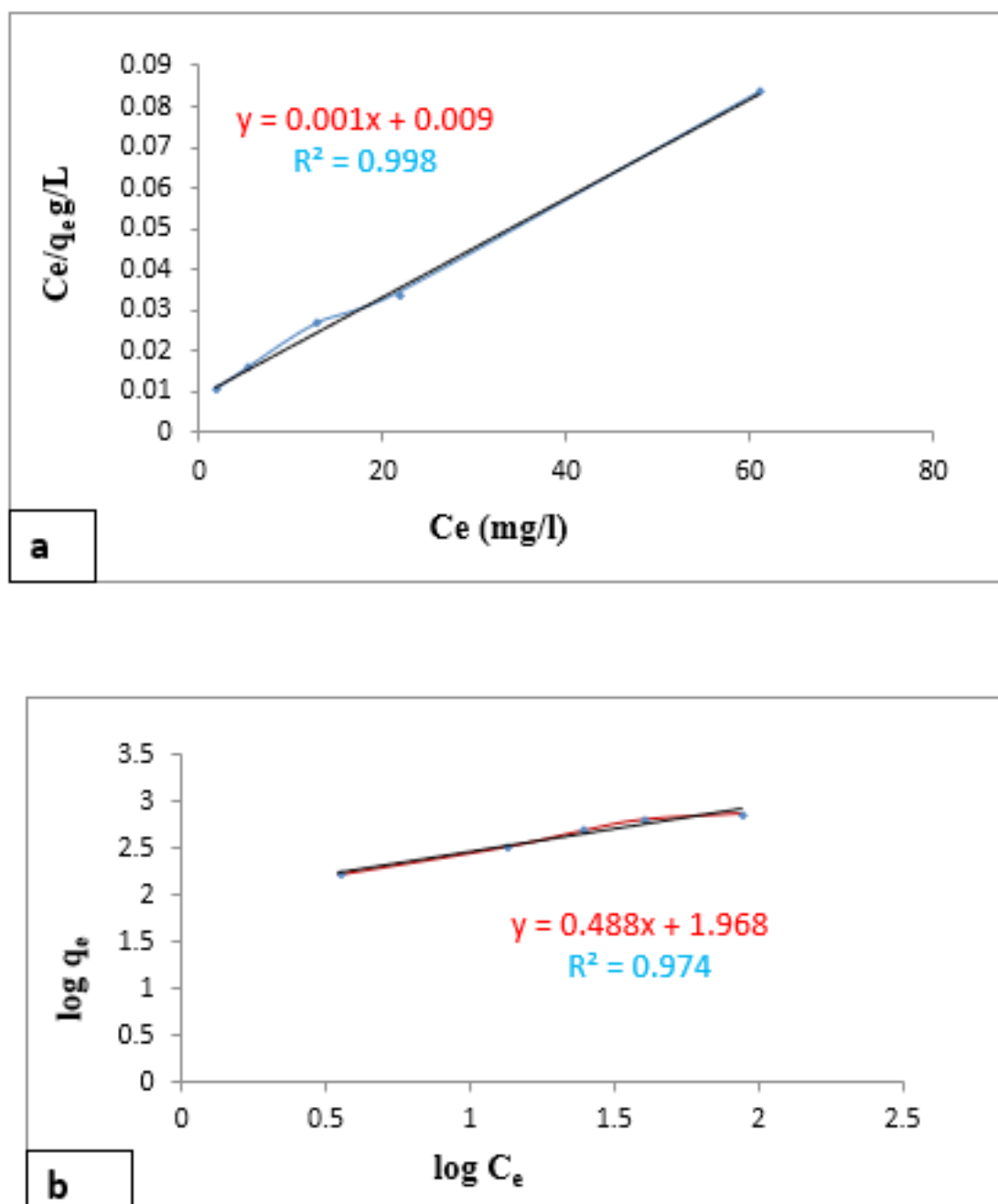


Fig. 11. a, Langmuir isotherm. b, Freundlich isotherm of Crystal violet.

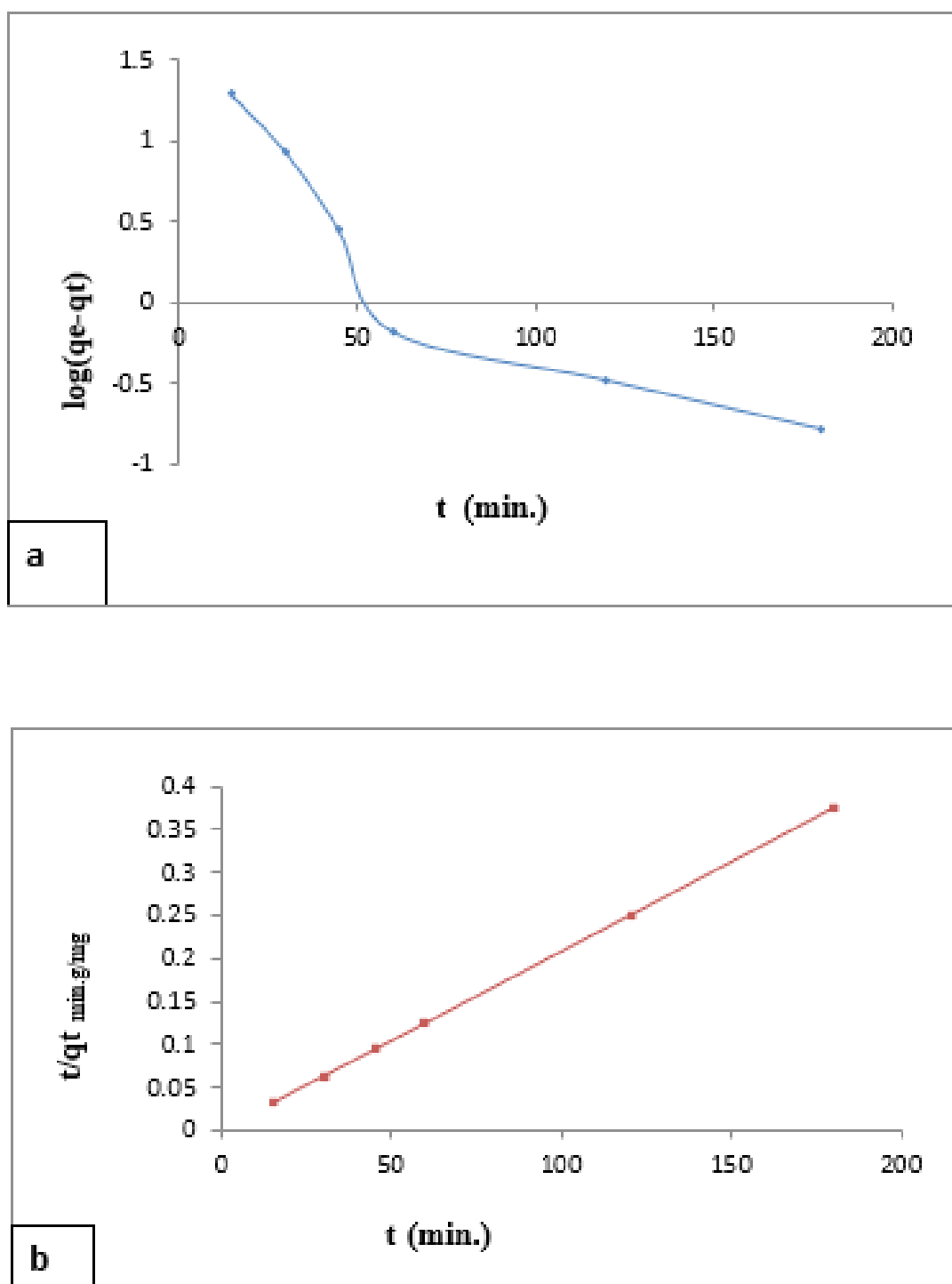


Fig. 12a. Pseudo first order. b, Pseudo second order of Crystal Violet.

adsorption intensity of the surface heterogeneity.

The experimental data of Crystal Violet dye adsorption was best fitted to Langmuir isotherm than Freundlich isotherm as screened in **Fig. 11a, b**. **Table 1** showed the calculated  $q_c$  comparison with experimental  $q_c$ , proved that Langmuir isotherm model is most appropriate as reported in another study [27, 28]. Two other parameters calculated from the Langmuir isotherm are worthy of discussion; the Langmuir constant ( $b$ ) and  $q_m$ . The parameter  $b$  speaks to the interaction escalated between the adsorbent and the adsorbate. Finally, it is possible from the Langmuir isotherm to predict if the adsorption of dye on the synthesized adsorbent were favorable or not. The taking after condition can be utilized to calculate a partition calculate (RL) (5):

$$RL = 1 / (1 + bC_0) \quad (5)$$

RL esteem uncovers the sort of the isotherm to be favorable ( $0 < RL < 1$ ), unfavorable ( $RL > 1$ ), straight ( $RL = 1$ ) or irreversible ( $RL = 0$ ). Herein, the RL value calculated for the Ch-StNPs composite was 0.03. Thus, the Crystal Violet dye adsorption on both adsorbent samples is favorable as reported in another study [7].

#### Adsorption kinetics

Adsorption kinetics gives important information about the mechanism of adsorption and permits comparing different adsorbents under special operational conditions for similar applications. Adsorption kinetic of Crystal Violet dye adsorbed onto StNPs citrate adsorbent were treated by pseudo-first-order and pseudo-second-order models, Eqs. (6) and (7), respectively:

$$\log (q_c - q_t) = \log q_c - k_1 t / 2.303 \quad (6)$$

$$t/q_t = 1/k_2 q_c^2 + t/q_c \quad (7)$$

where  $q_c$  and  $q_t$  are the adsorption capacity (mg/g) within the composite test at harmony and at any time  $t$ , separately.  $K_1$  is the rate steady of the pseudo-first-order, which was evaluated from the incline of the direct plots of  $\log (q_c - q_t)$  versus  $t$  **Fig. 12a**, and  $K_2$  is the rate consistent of the pseudo-second-order that was assessed from the captured of the direct plots of  $t/q_t$  versus  $t$  **Fig. 12b**, Adsorption kinetics of Crystal Violet dye onto StNPs citrate adsorbent are showing in **Fig. 12a,b**

and **Table 2**. The hypothetical values calculated for  $q_c$  utilizing the pseudo-second-order show were closer to the test  $q_c$  values **Table 6**. In contrast, the  $q_c$  values calculated using the pseudo-first-order model is not consistent with the experimental data. The correlation coefficient ( $R^2$ ) values calculated for that second kinetic model were higher than 0.99. These comes about recommended that the adsorption of precious stone violet onto StNPs citrate adsorbent were best spoken to by the pseudo-second-order condition, which is based on the presumption that the adsorption prepare may take put by rate-limiting step as detailed in another ponder [28, 29].

#### Thermodynamic studies

The thermodynamic behavior of Crystal Violet dye sorption onto StNPs citrate was investigated also by evaluation of free Gibbs energy ( $\Delta G^\circ$ ), enthalpy ( $\Delta H^\circ$ ) and entropy ( $\Delta S^\circ$ ) of the sorption system using Eqs. (8),(9) and (10):

$$K_d = C_e / q_c \quad (8)$$

$$\ln K_d = -\Delta G / RT = -\Delta H / RT + \Delta S / R \quad (9)$$

$$\Delta G = \Delta H - T\Delta S \quad (10)$$

where,  $K_d$  is the distribution constant,  $R$  (8.314 J/mol K) the all inclusive gas steady,  $C_e$  (mg/l) is the harmony concentration of color on adsorbent,  $q_c$  adsorption capacity at balance and  $T$  (K) the temperature.  $\Delta S^\circ$  and  $\Delta H^\circ$  were concluded from the incline and captured of Van't Hoff plot of  $\ln K_d$  vs.  $1/T$  **Fig. 13**. For Crystal Violet dye adsorbed onto StNPs citrate adsorbent the thermodynamic parameters in **Table 3** are calculated from Van't Hoff relation between  $\ln K_d$  vs.  $1/T$  as shown in **Fig. 13**, the obtained negative  $\Delta G^\circ$  values confirmed the dye sorption onto StNPs citrate to be spontaneous. The decrease in  $\Delta G^\circ$  values with increasing temperature indicated increase spontaneity of the sorption system at higher temperature. The positive esteem of  $\Delta H^\circ$  shown the sorption prepare was endothermic. The esteem of  $\Delta S^\circ$  illustrated arbitrariness at the solid-solute interface. The values of  $\Delta G^\circ$  and  $\Delta H^\circ$  as appeared in **Table 3**, indicate that the adsorption process was physisorption where the adsorbate adheres to the surface of adsorbent mainly via weak Van Der Waal's intermolecular interactions as reported in another study [30].

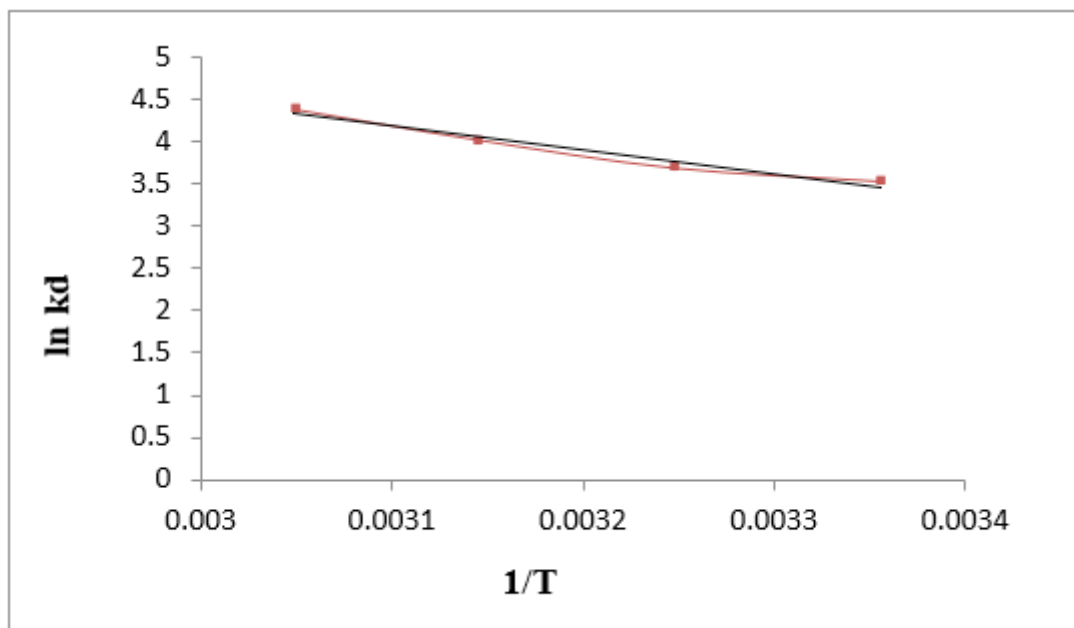


Fig. 13. Vant Hoff graph of Crystal Violet adsorption.

TABLE 1: Langmuir and Freundlich Isotherm for CV adsorption onto StNPs citrate adsorbent.

Adsorbent	T °C	$q_e$ (mg/g)	Langmuir Isotherm			Freundlich Isotherm			
			$q_m$ (mg/g)	b (L/mg)	$R^2$	Kf (L/g)	n	1/n	$R^2$
StNPs citrate	25	731.66	833.3	0.13	0.998	93.1	2.05	0.488	0.9748

TABLE 2: Pseudo first and pseudo second order parameters for Crystal Violet adsorption onto StNPs citrate adsorbent.

Crystal Violet adsorption on StNPs citrate		pseudo first order			pseudo second order		
$c_0$ (mg/L)	$q_e$ exp (mg/g)	$k_1$	$q_{ecal}$ (mg/g)	$R^2$	$k_2$	$q_e$ cal (mg/g)	$R^2$
300	478.5	0.027	0.04	0.8228	294.44	476.2	0.9999

TABLE 3: Thermodynamic parameters for Crystal Violet adsorption onto StNPs citrate adsorbent.

T (K)	$\Delta G$ (kJ mol <sup>-1</sup> )	$\Delta S$ (J mol <sup>-1</sup> K <sup>-1</sup> )	$\Delta H$ (kJ mol <sup>-1</sup> )
298	-9.3		
308	-8.3		
318	-7.3		
328	-6.3	100	23.5

## Conclusion

- 1- Synthesis of starch nano-particles through enzymolysis method is considered the most perfect way as term time, outlet nano measure starch and environment inviting. TEM and SEM images monitor round and polyhedral shape of native starch and StNPs and TEM image prove nano sized of prepared StNPs.
- 2- Novel anionic adsorbent is obtained from StNPs cross-linked with citric acid. The adsorbent is characterized by FT-IR that indicate ester linkage as a result of cross linking of StNPs with citric acid.
- 3- An anionic StNPs citrate is inspected as adsorbent for expulsion of Crystal Violet dye from watery arrangement. The comes about of adsorption prepare appeared that, the most elevated color evacuation is gotten at pH is 8.5, temperature 50 °C for 120 min.
- 4- The adsorption isotherm was best fitted to Langmuir that suggests a monolayer of adsorbate is formed on the surface of adsorbent. Furthermore, the adsorption of Crystal Violet dye was agreement with the pseudo- second -order kinetics that confirmed that the adsorption process occurred through physosorption phenomenon. Spontaneous, endothermic and randomness of adsorption process were proved by thermodynamic calculations.

## References

1. Aravamudhan, A., Ramos, D.M., Nada, A.A., Kumbar, S. G., Elsevier, *Natural and Synthetic Biomedical Polymers, Polysaccharides and Their Derivatives for Biomedical Applications*, Ch. 4, 67-89 (2014).
2. Huaxi Xiao, Fan Yang, Qinlu Lina, Qian Zhang, Weize Tang, Lin Zhang, Dong Xu, Gao-Qiang Liu, Preparation and properties of hydrophobic films based on acetylated broken-rice starch nanocrystals for slow protein delivery, *International Journal of Biological Macromolecules* 138, 556–564 (2019).
3. Sun, Q., Li, G., Dai, L., Ji, N., Xiong, L., Green preparation and characterization of waxy maize starch nanoparticles through enzymolysis and recrystallization. *J. Food chem.*162,223-228 (2014).
4. Tran, T., Athanassiou, A., Basit, A., Bayer, I., Starch-based bio-elastomers functionalized with red beetroot natural antioxidant, *Food Chemistry*,216, 324-333 (2017).
5. Le Corre. D., Bras, J., Dufresne,A., *Starch Nanoparticles: A Review*, ACS, *Biomacromolecules*, 11, 1139–1153 (2010).
6. El-Feky, G., El-Rafie MH, MA El-Sheikh, E El-Naggar, M., Hebeish A, Utilization of Crosslinked Starch Nanoparticles as a Carrier for Indomethacin and Acyclovir Drugs, *J. Nanomed. Nanotechnol.*, 6,1-9 (2015).
7. Gomes, R., C.A., Azevedo, N., Pereira, A., Muniz,E., Fast dye removal from water by starch-based nanocomposites, *J. Coll. and Interface Sci.*, 454, 200-209 (2015).
8. Huang, L., Xiao, C., Chen, B., A novel starch-based adsorbent for removing toxic Hg(II) and Pb(II) ions from aqueous solution, *J. Hazard. Mater.* 192, 832-836 (2011).
9. Qiao,D., Liu,H., Yu,L., Bao,X., P. Simon,G., Petinakis, E., Chen, L., Preparation and characterization of slow-release fertilizer encapsulated by starch-based superabsorbent polymer, *carbohyd. Polymer*, 147, 146-154 (2016).
10. Liu, X., Yan, L., Yin, W., Zhou, L., Tian, G., Shi, J., Yang, Z., Xiao, D., Gu, Z., Zhao, Y., A magnetic graphene hybrid functionalized with beta-cyclodextrins for fast and efficient removal of organic dyes. *Journal of Material Chemistry A* 2, 12296 –12303 (2014).
11. Robinson, T., Chandran, B., Nigam, P., Removal of dyes from a synthetic textile dye effluent by biosorption on apple pomace and wheat straw, *Water Research* 36, 2824–2830 (2002).
12. Kayan, B., Gozmen, B., Demirel, M., Gizir, A.M., Degradation of acid red 97 dye in aqueous medium using wet oxidation and electro-Fenton techniques, *Journal of Hazardous Materials*, 177, 95 –102 (2010).
13. Saeed, A., Sharif, M., Iqbal, M., Application potential of grapefruit peel as dye sorbent: kinetics, equilibrium and mechanism of Crystal Violet adsorption. *Journal of Hazardous Materials*,

- 179, 564–572 (2010).
14. Zhou, J., Tong, J., Su, X., Ren, L., Hydrophobic starch nanocrystals preparations through crosslinking modification using citric acid, *Int. J. of Biological Macromolec.*, 91, 1186-1193 (2016).
  15. Fumihiko, O., Noriaki, N., Naohito, K., Adsorption Capability of Cationic Dyes (Methylene Blue and Crystal Violet) onto Poly- $\gamma$ -glutamic Acid. *Chemical and Pharmaceutical Bulletin*, 65, 268- 275 (2017).
  16. Ho, Y.S., McKay, G., The sorption of lead (II) ions on peat. *Water Research*, 33, 578 – 584 (1999).
  17. Liu, C., Qin, Y., Li, X., Sun, Q., Xiong, L., Liu, Z., Preparation and characterization of starch nanoparticles via self-assembly at moderate temperature, *Biol. Macromol.*, 84, 354-360 (2016).
  18. Cheetham, N., Tao, L., Variation in crystalline type with amylose content in maize starch granules: an X-ray powder diffraction study, *J. carbohyd. chem.*, 36, 277-284 (1998).
  19. Yuan, H.Y., Nishiyama, Y., Wada, M., Kuga, S., Surface acylation of cellulose whiskers by drying aqueous emulsion, *Biomacromolecules*, 7, 696-700 (2006).
  20. Alshabanat, M., Alsenani, G., Almufarrij, R., Removal of Crystal Violet Dye from Aqueous Solutions onto Date Palm Fiber by Adsorption Technique. *J. Chem.*, 1-6 (2013).
  21. Jayganes, D., Tamilarasan, R., Kumar, M., Murugavelu, M., Sivakumar, V., Equilibrium and Modelling Studies for the Removal of Crystal Violet Dye from aqueous solution using eco-friendly activated carbon prepared from *Sargassum wightii* seaweeds, *J. Mat. Env. Sci.*, 8, 1508-1517 (2017).
  22. Kulkarni, M. R., Revanth, T., Acharya, A., Bhat, P., (2017), Removal of Crystal Violet dye from aqueous solution using water hyacinth: Equilibrium, kinetics and thermodynamics study, *Resource-Effici. Tech.*, 3, 71-77.
  23. Yakout, S. M., Ali, A. S., Removal of the Hazardous Crystal Violet Dye by Adsorption on Corn-cob-Based and Phosphoric Acid-Activated Carbon, *Particulate Science and Technology*, 33, 621–625 (2015).
  24. Shen, K., Gondal, M. A., Removal of hazardous Rhodamine dye from water by adsorption onto exhausted coffee ground, *J. Saudi Chem. Soc.*, 21, S120–S127 (2013).
  25. Tahir, N., Bhatti, H. N., Iqbal, M., Noreen, S., Bio-molecules composite with peanut hull waste and application for Crystal Violet adsorption, *bio. macromolec.*, 94, 210-220 (2016).
  26. Zhou, Y., Wang, M. Z. X., Min, Q.H.Y., Ma, T., Niu, J., Removal of Crystal Violet by a Novel Cellulose-Based Adsorbent: Comparison with Native Cellulose *Ind. Eng. Chem. Res.*, 53, 5498–5506 (2014).
  27. Pourjavadi, A., Hosseini, S. H., Seidi, F., Soleyman, R., Magnetic removal of crystal violet from aqueous solutions using polysaccharide-based magnetic nanocomposite hydrogels, *Polym Int.*, 62, 1038–1044 (2012).
  28. Wang, X. S., Liu, X., Wen, L., Zhou, Y., Jiang, Y., Li, Z., Comparison of Basic Dye Crystal Violet Removal from Aqueous Solution by Low-Cost Biosorbents, *Sep. Sci. Techn.*, 43, 3712–3731 (2008).
  29. Yan, H., Li, H., Yang, H., Li, A., Cheng, R., Removal of various cationic dyes from aqueous solutions using a kind of fully biodegradable magnetic composite microsphere, *Chem. Eng. J.*, 223, 402–411 (2013).
  30. Wang, X. S., Liu, X., Wen, L., Zhou, Y., Jiang, Y., Li, Z., Comparison of Basic Dye Crystal Violet Removal from Aqueous Solution by Low-Cost Biosorbents, *Sep. Sci. Techn.*, 43, 3712–3731 (2008).